

RESEARCH ARTICLE

Description of two new species of *Nostoc* (Nostocales, Cyanobacteria) from central Mexico, using morphological, ecological, and molecular attributes

Javier Carmona Jiménez¹  | Angela Caro Borrero¹  | Itzel Becerra-Absalón²  |
Elvira Perona Urizar³  | Kenia Márquez Santamaría¹  | Pilar Mateo Ortega³ 

¹Ecology and Natural Resources Department, Science Faculty, National Autonomous University of Mexico, Mexico City, Mexico

²Comparative Biology Department, Science Faculty, National Autonomous University of Mexico, Mexico City, Mexico

³Biology Department, Darwin 2, Science Faculty, Autonomous University of Madrid, Madrid, Spain

Correspondence

Itzel Becerra-Absalón, Comparative Biology Department, Science Faculty, National Autonomous University of Mexico, Exterior Circuit s/n, University City, Coyoacán, Mexico City 04510, Mexico.

Email: iba@ciencias.unam.mx

Funding information

Programa de Apoyo a Proyectos de Investigación e Innovación Tecnológica, Grant/Award Number: IN206821 and IN307219; CIANOPARK, Grant/Award Number: OAPN 2593/2020

Editor: D. Casamatta

Abstract

The present study describes two new *Nostoc* species, *N. montejanii* and *N. tlalocii*, based on a polyphasic approach that combines morphological, ecological, and genetic characteristics. The five investigated populations, including those from newly collected material from central Mexico, were observed to possess morphological features characteristic of the *Nostoc* genus. Results showed that both new species are strictly associated with running water, and they show clear differences in their habitat preferences. The 16S rRNA gene sequences of the five strains displayed between 98% and 99% similarity to the genus *Nostoc sensu stricto*. The 16S rRNA gene phylogenetic analyses inferred using Bayesian inference, maximum likelihood, and parsimony methods, placed these five strains in two separate clades distinct from other *Nostoc* species. The secondary structures of the 16S–23S internal transcribed spacer rRNA region in the two new species showed >10.5% dissimilarities in the operons when compared with other *Nostoc* species. In addition, clear morphological differences were observed between the two Mexican species, including the color of the colonies (black in *N. montejanii* and green in *N. tlalocii*), the size of the cells (greater in *N. montejanii*), and the number of polyphosphate granules present in the cells (one in *N. montejanii* and up to four in *N. tlalocii*).

KEYWORDS

16S rRNA gene, 16S–23S ITS, benthic cyanobacteria, ecology, new species, *Nostoc*, taxonomy

INTRODUCTION

The genus *Nostoc* (Order: Nostocales) is a conspicuous group of freshwater cyanobacteria that occurs widely and abundantly in lotic ecosystems throughout

the world (Dodds et al., 1995). Recently, Komárek et al. (2014) classified the Nostocales order into 12 families based on morphological, molecular, and ecological features. This classification employed the polyphasic taxonomic approach, which involves the integration of

Abbreviations: BI, Bayesian inference; BLAST, basic local alignment search tool; CUME, Cuenca de México; DIN, dissolved inorganic nitrogen; DO, dissolved oxygen; FCME, freshwater algal herbarium; ITS, internal transcribed spacer; K_{25} , specific conductivity; MCL, maximum composite likelihood; MCMC, Markov chain Monte Carlo; ML, maximum likelihood; MP, maximum parsimony; NCBI, National Center for Biotechnology Information; OTU, operational taxonomic unit; PCR, polymerase chain reaction; PSRF, potential scale reduction factor; RNA, ribonucleic acid; SPR, subtree-pruning-regrafting; SRP, soluble reactive phosphorous; T , temperature; TEM, transmission electron microscope; UNAM, Universidad Nacional Autónoma de México.

This is an open access article under the terms of the [Creative Commons Attribution-NonCommercial-NoDerivs](https://creativecommons.org/licenses/by-nc-nd/4.0/) License, which permits use and distribution in any medium, provided the original work is properly cited, the use is non-commercial and no modifications or adaptations are made.

© 2023 The Authors. *Journal of Phycology* published by Wiley Periodicals LLC on behalf of Phycological Society of America.

various tools (e.g., life cycles, morphology, ultrastructure, physiology, molecular biology, ecology, etc.) to improve and delimit taxonomic classifications. This taxonomic approach is supported by the species concept as proposed by Komárek (2006): “a species is a group of populations (+ strains) which belong to one and the same genotype (genus), should be characterized by stabilized phenotypic features that are definable, have distinct limits to their variation, AND have the same ecological demands” (p. 360). The genus *Nostoc* is included in the family Nostocaceae, but its systematic position has been controversial due to similarities in morphology and life cycles. As such, the great diversity within this group has led to a polyphyletic grouping of its taxa (Cai et al., 2020). Currently, the genus *Nostoc* comprises a complicated and widely distributed group with many morphotypes and genotypes, with over 246 species listed in AlgaeBase (Guiry & Guiry, 2023, continuously updated). This phenotypic plasticity, seen both in the field and in cultured samples, continues to make taxonomy difficult, and many *Nostoc*-like genera have recently been re-categorized (Bagchi et al., 2017; Cai, Li, Yang, et al., 2019). Komárek suggested that typical *Nostoc* likely comprises only the types producing macroscopic colonies with a distinct morphology based on the *Nostoc commune* type and, consequently, only includes species that are recognizable according to characteristic markers (Johansen & Casamatta, 2005). The *Nostoc* genus has been known to be genetically heterogeneous and in need of a modern taxonomic revision that combines both molecular and morphological approaches (Komárek et al., 2014). Recent phylogenetic studies based on 16S rRNA gene sequences have confirmed that strains assigned to *Nostoc* do not form a monophyletic group (Hentschke et al., 2017). In response, the following taxonomic revisions were carried out by different research groups, with interesting results that reveal the existence of 10 new genera separated from *Nostoc sensu stricto*: *Halotia* (Genuário et al., 2015), *Mojavia* (Řeháková et al., 2007), *Desmonostoc* (Hrouzek et al., 2013), *Aliinostoc* (Bagchi et al., 2017), *Komarekiella* (Hentschke et al., 2017), *Compactonostoc* (Cai, Li, Yang, et al., 2019), *Desikacharia* (Saraf et al., 2019), *Violetonostoc* (Cai et al., 2020), *Purpleonostoc* (Cai & Li, 2020), and *Pseudoallinostoc* (Lee et al., 2021). These taxonomic decisions were largely possible due to sequencing of the 16S rRNA genes and internal transcribed spacer (ITS) rRNA regions since morphological similarity is very high (Cai, Li, Geng, et al., 2019). Of note, however, is that genera within the Nostocacea family present molecular similarities greater than the 95% threshold established in microbiology (Stackebrandt & Ebers, 2006), with some Nostocales groups being up to 99% similar (Cai, Li, Geng, et al., 2019).

In ecological terms, some species of *Nostoc* possess several morphological, reproductive, and physiological

adaptations potentially linked to unidirectional current velocity (Mollenhauer, 1988). For example, Mateo et al. (2006) described morphological adaptations related to the confluent and large amounts of mucilage surrounding the filaments, colony aggregation with a compact and efficient attachment system, and mucilage protection for humidity retention and assimilation. Examples of reproductive adaptations include akinetes and/or hormogonia formations (Dodds et al., 1995), which can disperse and form new colonies when environmental conditions become favorable or otherwise stay in a cryptobiotic state.

Nostoc morphotype populations have been collected in several central Mexican streams from siliceous and calcareous tropical waters (Carmona-Jiménez et al., 2022; Montejano et al., 2004). Komárek (2013) reported only four species that live in riverbeds, the majority from temperate environments—*N. verrucosum*, *N. membranaceum*, *N. parmelioides*, and *N. letestui*. Consequently, populations from Tambaque, San Luis Potosí have been identified based on morphological characters as *N. verrucosum* (Cartajena et al., 2020), while populations from San Miguel have been considered to be *N. parmelioides* (Rodríguez-Flores & Carmona-Jiménez, 2018). However, the taxonomical, ecological, and genetic characterizations of these populations are poorly known. The present investigation aims to (i) describe ecological limits, (ii) assess morphological diversity, including variation in nature and culture, and (iii) genetically analyze the 16S rRNA gene sequence and the 16S–23S ITS rRNA region secondary structure to establish phylogenetic relations. The results of this polyphasic study show that these populations from central Mexico represent new species.

MATERIALS AND METHODS

Ecological characterization

Five populations of *Nostoc* were sampled from the central region of Mexico (19°13'–21°41'N, 99°02'–99°28'W) in altitudes from 395 to 3,349m (Figure 1). Cover percentage was estimated using the quadrant technique (Necchi et al., 1995) in river segments measuring 10m long, and five samples from each segment were obtained. Part of the samples were preserved alive for observation and subsequent cultivation in the laboratory, while another part was preserved in 4% formaldehyde (Holmgren et al., 1990) to be deposited in the Freshwater Algal Herbarium (FCME). Herbarium abbreviations follow the online Index Herbariorum (Thiers, 2023).

Temperature, pH, dissolved oxygen (DO) content, and specific conductivity were measured with a YSI PRODSS-multiparameter. To further investigate

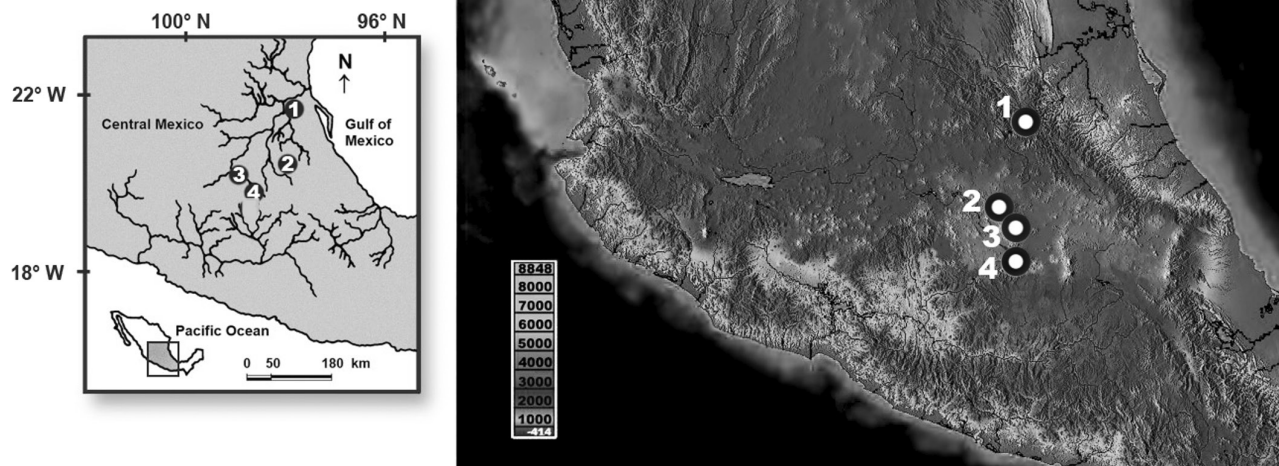


FIGURE 1 Distribution of *Nostoc* populations in streams from central Mexico. Group I, *Nostoc montejanii*: (1) Tambaque spring. Group II, *N. tlalocii*: (2) Iturbide dam, (3) Monte Alegre spring, (4) Iturbide spring.

water chemistry, 1-L samples were taken and analyzed for calcium and nutrient concentrations in the field within 1 h of collection using a DRELL 3000 laboratory (Hach Company). These analyses are adapted from the *Standard methods for the examination of water and wastewater* (American Public Health Association, 1995). Dissolved inorganic nitrogen (DIN) was calculated as the sum of the three inorganic nitrogen forms in water. Ammonium was measured with a colorimetric analysis following the Nessler method (detection limit: $0.1 \text{ mg} \cdot \text{L}^{-1}$), reading the absorbance at 425 nm. When values were close to the detection limits, the salicylate method was used (detection limit: $0.01 \text{ mg} \cdot \text{L}^{-1}$), with readings at 655 nm. Nitrate was similarly measured with a colorimetric analysis following a modification of the cadmium reduction method, using gentisic acid instead of 1-naphthylamine (detection limit: $0.5 \text{ mg} \cdot \text{L}^{-1}$), with absorbance readings at 500 nm. The low-range method (up to $0.5 \text{ mg} \cdot \text{L}^{-1}$) is an expanded modification of the former that employs a chromotropic acid indicator (detection limit: $0.05 \text{ mg} \cdot \text{L}^{-1}$), reading at the same wavelength. Nitrite was determined colorimetrically using chromotropic and sulphanilic acids as indicators (detection limit: $0.01 \text{ mg} \cdot \text{L}^{-1}$), with absorbance readings at 500 nm. Dissolved inorganic nitrogen was calculated as the sum of nitrite, nitrate, and ammonium. Soluble reactive phosphorous was estimated colorimetrically with a modification of the molybdenum blue procedure, provided by Phos Ver 3 (detection limit: $0.01 \text{ mg} \cdot \text{L}^{-1}$), with absorbance readings at 890 nm. All measurements were taken in duplicates.

Strain sampling, isolation, and culturing

Samples used in this study were isolated from the five sites comprising the study area (Table 1). Unialgal filaments from the cyanobacterial samples were isolated by Pasteur pipette under the Olympus SC31 microscope and then cultured in petri dishes containing BG11-agar medium. All isolates were subsequently cultivated at 25°C under a 12:12 h (light:dark) cycle with a photon flux density of $40\text{--}45 \mu\text{mol} \cdot \text{m}^{-2} \cdot \text{s}^{-1}$ from white, fluorescent lamps. The unialgal cultures were used for morphological observations and life cycle studies.

Morphological analyses

Biological characteristics of all populations (natural and culture samples) were analyzed minimally in triplicates. Quantitative and qualitative morphological measurements were made in 50 replicate filaments, with the number of replicates determined using the equation: $n = (\text{SD}/\text{SE})^2$, where SD = standard deviation, SE = (predeterminate) standard error (in this case, 0.05) and x = average (Southwood, 1978). A BX51 Olympus microscope equipped with a SC35 photomicrographic system was used for observations, measurements, and photographing samples. In each population, morphological characters, previously considered in relevant studies to be of taxonomic importance at generic and specific levels, were measured (Komárek, 2013). For ultrastructural analysis by transmission electron microscope (TEM),

TABLE 1 Physical and chemical characteristics of the *Nostoc* population in streams from central Mexico.

Site, altitude and date	Location (latitude North, longitude West) and geological origin	T (°C)	pH	K ₂₅ (μS·cm ⁻¹)	DO (mg·L ⁻¹)	Current velocity (m·s ⁻¹)	SRP (mg·L ⁻¹)	Ammonium (mg·L ⁻¹)	Nitrite (mg·L ⁻¹)	Nitrate (mg·L ⁻¹)	DIN (mg·L ⁻¹)
1. Tambaque 395 22.03.2019	21°41'08" 99°02'36" Calcareous	23.5	7.0	1528	8.4	0.80	0.02	0.060	0.002	0.035	0.097
2. Iturbide dam 3205 18.12.2018	19°32'05" 99°27'38" Basaltic	9.5	7.5	58	7.9	0.18	0.445	0.010	0.025	0.001	0.036
3. Monte Alegre spring 3349 31.01.2018	19°13'49" 99°17'22" Basaltic	7.6	8.0	52	8.9	0.55	0.275	0.095	0.011	0.087	0.193
4. Iturbide spring 3339 12.12.2018	19°31'45" 99°28'58" Basaltic	9.3	6.9	38	7.6	0.06	0.395	0.080	0.003	0.010	0.093

Abbreviations: DIN, dissolved inorganic nitrogen; K₂₅, specific conductivity; SRP, soluble reactive phosphorous; T, temperature.

samples were prepared and stained with lead citrate (Reynolds, 1963), washed 3 times with a buffer of sodium phosphate 0.1 M pH 7.2 (used throughout the procedure), and damper fixed in 3.1% glutaraldehyde for 3 h at 4°C. The samples were washed 3 times and included in bacteriological agar in 4% buffer. After fixation, 1- to 2-mm blocks were placed in osmium tetroxide buffer for 2 h at 4°C. Samples were then dehydrated with ethanol and embedded in Spurr resin (Spurr, 1969), sectioned on a Reichert-Jung Ultracut E Ultratome, stained with lead citrate (Reynolds, 1963), and viewed under a JEOL 1010 TEM.

RNA extraction and sequencing

RNA was extracted from mat samples using a QIAGEN DNeasy UltraClean Microbial Extraction Kit. Frozen mat samples were thawed at room temperature for 0.5 h, and 0.15 g of mat removed for RNA extraction. The RNA extraction followed manufacturer's protocol, except the cell lysis step was modified. The samples were pretreated to facilitate cell rupture, which consisted of three freeze/heat cycles with liquid nitrogen and heating in an AccuBlock (Labnet International Inc.) at 65°C. Between each of the cycles, a drill and a plastic pistil were used. The presence of RNA was confirmed by electrophoresis (0.8% agarose gel), and its concentration was measured in a microplate spectrophotometer (Epoch: BioTek Instruments Inc.).

Amplification of the 16S rRNA gene was performed by PCR using the Biometra TOne Thermal Cyclers thermocycler (Analytik Jena). The following reaction master mix was used: milli-Q water, 10× PCR buffer, Cl₂Mg (50 mM), deoxyribonucleotide triphosphate (50 μM dNTP), bovine serum albumin (BSA, 0.1%), DNA polymerase (Ultratools DNA Polymerase: 1 unit·μL⁻¹, and Thermoscientific DreamTaq DNA Polymerase: 20 and 500 unit·μL⁻¹). The primers (10 pM) used were the oligonucleotides 27F (5'-AGAGTTTG ATCCTGGCTCAG-3'; Wilmette et al., 1993) and 23Sr (5'-CTTCGCCTCTGTGTGCCTAGGT-3'; Lepère et al., 2000), using milli-Q water as negative control. Following this, an agarose gel electrophoresis (1.5%) was performed to reveal the PCR product. Once the RNA bands were obtained, the PCR product was purified with the Wizard SV Gel and PCR Clean-up System Kit (Promega). Subsequently, the cloning procedure using the Pgem-t Easy Vector System Ligation Kit (Promega) was carried out to ensure the greatest biological representativeness of the algal consortium. The transformation process was carried out using 100 μL of the competent bacteria strain *Escherichia coli* (DH5a). The transformed bacteria were inoculated (250 μL) in Petri dishes with solid LB medium (Bertani, 1951), ampicillin (0.1 mg·mL⁻¹), X-Gal: 5-bromo-4-chloro-3-indolyl-β-D-galactopyranoside (0.04 mg·mL⁻¹) and IPTG:

isopropyl- β -D-1-thiogalactopyranoside (0.5 mM). The cultures were incubated at 37°C for 24 h. The positive clones (presence of the insert) were recognized by their white coloration and were reseeded in LB medium. Negative clones (blue colonies without insert) were discarded. The presence of the insert was confirmed by PCR and electrophoresis. The reaction master mix used was the following: milli-Q water, 10 \times PCR buffer, Cl₂Mg (50 mM), deoxyribonucleotide triphosphate (50 μ M dNTP), and DNA polymerase (Ultratools DNA Polymerase: 1 unit- μ L⁻¹ and Thermoscientific DreamTaq DNA Polymerase: 20 and 500 unit- μ L⁻¹). As primers (10 pM) the oligonucleotides T7 (5'-TAATACGA CTCACTATAGGG-3') and SP6 (5'-ATTTAGGTGAC ACTATAG-3') were used.

Once the presence of the insert was confirmed, the transformed bacteria were cultured in liquid LB medium with ampicillin at 37°C and horizontal movement of 250 rpm for 24 h. Afterward, the extraction and purification of the plasmids was carried out with the Wizard Plus SV Minipreps DNA Purification System Kit (Promega). Once the plasmid DNA was obtained, its concentration was measured (Epoch: BioTek Instruments Inc.) to be sent for sequencing.

The sequencing process was carried out at the DNA Synthesis and Sequencing Unit (USSDNA) of the Institute of Biotechnology-UNAM (National Autonomous University of Mexico). The primers used for sequencing were T7 (5'-TAATACGACTCACTATAGGG-3'), SP6 (5'-ATTTAGGTGACACTATAG-3') and 684F (5'-GTGTA GCGGTGAAATGCGTAGA-3'; Mateo et al., 2011).

The sequences obtained were assembled using the BioEdit 7.2 program (Hall, 1999) and compared with sequence information available in the National Center for Biotechnology Information (NCBI) by BLAST analysis (<http://www.ncbi.nlm.nih.gov/BLAST>). Those sequences with identity percentages above 98% similarity and some sequences of genera and species belonging to nearby taxonomic group were considered for the construction of different sequence databases with which the phylogenies were built (<http://www.cyanodb.cz/> and <https://www.ncbi.nlm.nih.gov/>).

Phylogenetic analyses

Generated sequences were compared with available sequence information in the NCBI database using BLAST, and the most related sequences were selected for inclusion in the phylogenetic analyses. Additional sequences from GenBank were selected based on morphological classification criteria so that sequences from several Nostocales families were represented, including many of the recently described genera in the order. The taxa used in the 16S rRNA gene phylogenetic analyses included a total of 417 operational taxonomic units (OTUs) with *Chroococcidiopsis thermalis*

as an outgroup. A multiple-sequence alignment was performed using ClustalW (Thompson et al., 1994), and the alignment (Appendix S1 in the Supporting Information) was visually checked and corrected using PhyDE-1 v0.9971 (Müller et al., 2019). Bayesian inference (BI), maximum likelihood (ML), and maximum parsimony (MP) analyses were performed using partial 16S rRNA gene sequences containing a maximum of 1629 characters that included both nucleotides and indels.

Bayesian inference was conducted with MrBayes XSEDE V3.2.6 (Ronquist et al., 2012) through the CIPRES Science Gateway, applying the GTR+G+I model of nucleotide substitution and running a total of 10 million generations. The BI analysis had an estimated sample size (ESS) exceeding 300 for all parameters, well above the typically accepted value of 200 deemed sufficient by phylogeneticists (Drummond et al., 2006). The final average standard deviation of split frequencies was <0.04. The potential scale reduction factor (PSRF) value for all the estimated parameters in the BI analysis was 1.00, indicating that convergence of the MCMC chains was statistically achieved (Gelman & Rubin, 1992).

Maximum likelihood (ML) was conducted with MEGA7 (Kumar et al., 2016) and applied the Kimura 2-parameter model of nucleotide substitutions, with 1000 bootstrap iterations. Initial tree(s) for the heuristic search were obtained automatically by applying Neighbor-Joining and BioNJ algorithms to a matrix of pairwise distances estimated using the Maximum Composite Likelihood (MCL) approach and then selecting the topology with superior log likelihood value. A discrete Gamma distribution was used to model evolutionary rate differences among sites (five categories; +G, parameter=0.3604). The rate variation model allowed for some sites to be evolutionarily invariable ([+I], 24.57% sites). The tree is drawn to scale, with branch lengths measured in the number of substitutions per site.

Maximum parsimony (MP) analysis was conducted using PAUP v.4b10; the indels were counted as a fifth base. The length of the most parsimonious tree was 5759; of the 1629 characters only 586 were parsimony informative. The MP tree was obtained using the tree-bisection-reconnection (TBR) algorithm, with search level=1, indicating that the initial trees were obtained by the random addition of sequences (10 replicates). One thousand bootstrap replicates were run.

Bootstrap values for both the ML and MP analyses and posterior probability values of BI were mapped onto the BI tree (general tree, Figure 2a) and MP tree (*Nostoc sensu stricto* clade, Figure 2b).

The percent identity was calculated among the 33 strains, to *Nostoc sensu stricto* and to morphologically similar genera to *Nostoc*, based on 16S rRNA gene sequences. These sequences were trimmed so that the majority of sequences were of the same size (1100 bp),



FIGURE 2 (a) Bayesian Inference analysis of 415 Nostocales OTUs plus *Chroococcidiopsis thermalis* as the outgroup based on a 1629 nucleotide alignment of partial rRNA gene sequences. Support values (bootstrap for MP/ML and posterior probabilities for BI) are mapped onto nodes, in bold and black highlight *Nostoc sensu stricto* clade. (b) Maxima Parsimony analysis is shown, support values (bootstrap for MP/ML and posterior probabilities for BI) are mapped onto nodes, in light gray square *N. tlaocii* and dark gray square *N. montejanii*. Asterisk (*) indicates bootstrap and posterior probabilities values of 100%, and only values >50% shown.

and the analysis was performed with the *p*-distance command in MEGA7 (Kumar et al., 2016).

An alignment of 26 sequences of the 16S–23S ITS rRNA region for *Nostoc sensu stricto* species, including our strains, was constructed in Clustal W, with constraints that forced alignment of all conserved domains (helices, Box-A, tRNA genes, etc.). From this alignment, we determined two ribosomal operons to be present in *Nostoc*, with most sequences possessing both tRNA genes, but some having an operon without tRNA genes. A new alignment was made only of operon sequences with tRNAs (14 strains and 700 characters);

the *p*-distances of ITS rRNA region sequences were calculated using the SHOWDIST command in PAUP 4.0 beta version 10, and MP analysis was conducted using PAUP v. 4b10, counting indels as a fifth base and running 10,000 bootstrap replicates. All phylogenies in this paper were visualized in Fig Tree and subsequently edited in Corel Draw.

The hypothetical secondary structures of conserved domains in the 16S–23S ITS rRNA region, including D1–D1', Box-B, V2, and V3 helices, were derived using M-fold (Zuker, 2003). Separate structures for operons with two tRNA genes and those with no tRNA genes

were determined. Internal transcribed spacer rRNA region structures of other closely related taxa were determined and reported for comparative purposes. Differences between all described taxa and the two Mexican strains were indicated by using open and closed circles on variable nucleotides.

RESULTS

Descriptions and taxonomic proposals

According to our results, the populations from two different geographic areas in central Mexico presented unique characteristics that differentiated them from other *Nostoc* species, and as such we describe them as new species.

Nostoc montejanii J. J. Carmona-Jiménez, Caro-Borrero, A. et Becerra-Absalón I. sp. nov. (Table 2, Figure 3)

Description: Colonies spherical and hard to the touch, start dark and become grayish green. Filaments released by the colony rupture, covered with compact and stratified sheath, and the filaments or multiseriate filaments densely entangled to form young colony. Within the colony, filaments segmented into several small groups that show compartmentalization of mucilage, in some cases forming aseriated filaments, later forming small and compact spherical colonies. Consequently, older colonies consist of aggregations of microcolonies, similar to a beehive. Eventually, the older colony breaks to release these small colonies. Sheath thick, colorless. Vegetative cells short barrel-shaped to subspherical, or oblong, 3.1–5 µm long and 4–6.1 µm wide. One prominent polyphosphate granule per cell and plain fascicular thylakoids. Heterocytes spherical, with a diameter of 3.3–5.2 µm. Akinetes not observed during cultivation.

Type locality: Isolated from Tambaque stream, Aquismon municipality, San Luis Potosí State, Mexico.

Holotype here designated: MEXICO. San Luis Potosí State, from calcareous stream, 21°41'08" N, 99°02'36" W, collected 22 March 2019, collector's name Javier Carmona. Collector number FCME PA4350, field sample preserved in 4% formaldehyde, deposited in the collection of the Herbarium at the Facultad de Ciencias, FCME, at Universidad Nacional Autónoma de México (UNAM).

Etymology: *montejanii* = Refers to Professor Gustavo Montejano Zurita, prominent Mexican phycologist pioneer.

Habitat: Epilithic in high-current velocity, shallow calcareous tropical streams.

Nostoc tlalocii J. J. Carmona-Jiménez, Caro-Borrero, A. et Becerra-Absalón I. sp. nov. (Table 2, Figure 4)

Description: Colonies spherical or ear-shaped, which represents a transformation due to chironomids that grow associated in the colony and probably use it as refuge and food in the larval stage. Colony gray-green in color throughout its development. Filaments released by the colony rupture, covered with sheath, and the filaments densely entangle to form young colony. Within the colony, the filaments are segmented into several small groups that show mucilage compartmentalization, which later form small spherical colonies. Eventually, each colony is occupied by a chironomid larva that modifies its spherical shape to a compressed ear-shaped cavity. Vegetative cells short, barrel-shaped to subspherical, or oblong, 1.4–5.0 µm long and 1.5–4.2 µm wide. Several small polyphosphate granules per cell. Heterocytes spherical, with a diameter of 3.5–4.6 µm. Akinetes were not observed during cultivation.

Type locality: Isolated from Monte Alegre stream, Mexico City, Mexico.

Holotype here designated: MEXICO. Mexico City, from basaltic stream, 19°13'49" N, 99°17'22" W, collected 31 February 2018, collector's name Javier Carmona. Collector number FCME CUME100, field sample preserved in 4% formaldehyde, deposited in FCME, at Universidad Nacional Autónoma de México (UNAM).

Etymology: *tlalocii* = Refers to "Tlaloc," the god of rain and prosperity in the Aztec religion that was worshiped in the region during pre-Hispanic times.

Habitat: Epilithic in high current velocity, shaded basaltic streams.

Ecology and distribution

The four populations presented visible growth with a relevant percentage coverage (35%–90%). The physical and chemical parameters show two distinct groupings (Table 1, Figure 1). Group one contains four populations from shallow mountain streams with low temperatures (7.6–9.5°C), low ionic content (specific conductivity 38–58 µS·cm⁻¹), high oxygenated water (7.6–8.9 mg·L⁻¹), low nutrients (soluble reactive phosphorous 0.275–0.445 mg·L⁻¹ and DIN 0.036–0.193 mg·L⁻¹), and relatively large measurements of current velocity (0.06–0.55 m·s⁻¹). *Nostoc* colonies in the Monte Alegre and Iturbide springs sites contained Chironomidae larvae, which modify their architecture to the appearance of an "ear." The second group contains the downland and calcareous Tambaque population, which are from warm water (23.5°C) highly mineralized

TABLE 2 Morphological characteristics (average, minimum, and maximum, $n=50$) of the *Nostoc* populations in streams from central Mexico and other species of the genus (Cai et al., 2021; Komárek, 2013; Mesfin et al., 2020; Singh et al., 2020).

Species	Site	Cover (%)	Growth form and color
<i>Nostoc montejanii</i>	1. Tambaque PA	75 60–90	Compact colony Black
<i>Nostoc tlalocii</i>	2. Iturbide dam CUME	35 20–45	Mucilaginous colony Brown
	3. Monte Alegre spring CUME	60 35–85	Compact colony and MIB's associates Brown
	4. Iturbide spring CUME	40 15–60	Compact colony and MIB's associates Brown
<i>Nostoc verrucosum</i>	Temperate rivers	—	Spherical to hemispherical and lobate Olive-green to dark brown
<i>Nostoc calcicola</i>	Wet soils and wetted rock walls	—	Irregular, flat, gelatinous Olive-green, grayish blue-green or yellowish green
<i>Nostoc carneum</i>	Attached to submersed substrate. Temperate zones	—	First spherical, later vesicular, lobate or irregularly clustering, gelatinous, fine, macroscopic Grayish, reddish-violet, brownish, olive-green or grayish blue-green
<i>Nostoc commune</i>	Subaerophytic, on wet sand soils, grasslands, semideserts, edge of ways Temperate and tropical regions	—	Gelatinous±spherical Latter irregularly flattened Olive-green yellow green to brown up to dark brown
<i>Nostoc desertorum</i>	Biological soil crust	—	Microscopic free-living Agar: conglomerations of small, spherical to lobate Dark green and become yellow-green to gray-green
<i>Nostoc edaphicum</i>	Subaerophytic on soils	—	Microscopic spherical or oval Mucilage colorless or yellow-brownish
<i>Nostoc favosum</i>	Free-living on edge of a stream in the soil	—	Spherical Yellow to gray-green
<i>Nostoc flagelliforme</i>	Wetted sandy soils in deserts and mountains	—	Macroscopic filamentous threads, irregular net-like colonies on soil substrate Olive-green up to dark blue-green and blackish
<i>Nostoc indistinguendum</i>	Desert soil	—	Microscopic spherical to irregulars Agar: up to macroscopic, gelatinous no satellite colonies Green
<i>Nostoc lichenoides</i>	Desert soil	—	Microscopic in the thallus of <i>Collema tenax</i> Agar: starting microscopic and becoming a macroscopic thallus, spherical to lobate Dark green to yellowish-brown
<i>Nostoc parmelioides</i>	Temperate rivers	—	Spherical to slightly flattened Brown
<i>Nostoc piscinale</i>	Small, stagnant, unpolluted water reservoirs Cosmopolitan	—	Fine, thin, mucilaginous, at first±spherical Latter irregularly clustered Brownish, yellow-brownish or dirty olive green
<i>Nostoc punctiforme</i>	Subaerophytic, attached to the substrate European temperate zones	—	Small, spherical Dark blue-green or blackish Latter blackish gelatinous mass
<i>Nostoc sphaeroides</i>	Stony bottom of clear northern lakes in Europe and North America	—	Spherical, hemispherical or irregularly oval Olive-green, grayish-green or pale blue-green
<i>Nostoc sphaericum</i>	Among water plants and mosses Mediterranean climate	—	Spherical or slightly oval Olive-green, brown, yellow-brown or violet-brown
<i>Nostoc membranaceum</i>		—	Spherical to thin membranes Hyaline to yellowish-brown
<i>Nostoc mirabile</i>	Free-living on wet rocky	—	Aggregation of spherical colonies Dark green
<i>Nostoc neufordense</i>	Soil or seepage	—	Hemispherical; with true branching Green
<i>Nostoc letestui</i>	On stones in streams	—	Hemispherical to crustaceous mats
<i>Nostoc oromo</i>	Microbiotic crust	—	Spherical to oblong or irregular Bright blue-green to olive

Height colony (cm)	Cell length (μm)	Cell width (μm)	Heterocyte diameter (μm)	Polyphosphate granules in the cell
1.6	4.60	4.79	4.5	1
1.2–2.0	3.1–5	4.0–6.1	3.3–5.2	
4.3	2.5	3.49	4.1	1–3
1.3–4.6	1.8–3.8	2.0–4.0	3.5–4.5	
1.5	3.3	2.7	4.3	1–4
0.5–2.1	1.4–5.0	1.5–3.5	3.8–4.6	
1.8	2.5	3.49	4.0	1–3
0.8–2.2	1.7–3.8	2.0–4.2	3.2–4.4	
>5	3–4.5 (6)	6	7×5	—
Agglomerations >10				
Up to 5		2.5–3	4–5	—
—	6–8	3–4	4–6	—
Up to 1.5. Several cm in diameter	3–5.5	4–4.3	5.5–8.4×5–8	—
Up to 0.0045	40–45	30–35	3–8×2–8	—
0.047	—	3–4.2	—	—
	2.7–3.1×3.8	2.7×4.4–4.6	2.8×4.3–4.9	—
0.2–0.5		4–5	5–6	—
—	2–5	2–5	3–7×2–6	—
	3–5	3–5	3–6×2–6	—
2	2.2–5	3.5–5.2	4.8–6.5×4.8–7	—
—	—	3.5–4	5–6	—
0.1 up to 0.2. Several cm large	—	3–5	4–6.5	—
Usually, 1 up to 3–4	4–7	4–6	6–7	—
2–3	3.5–5	3.5–5	6–8×4–6	—
100–125	5–8	4.6–5.2	5.8–6.4	—
—	2.8–3.4×3.7	3.0–3.5×3.9	3.3–3.9–4.2×3.6–4.1–4.8	—
—	3.41–5.68	2.53–3.61	4.69–5.9×3.24–3.56	
—	2	5.5–6.5	10	
0.05	4–6	—	Very rare 4–6×3–4	1

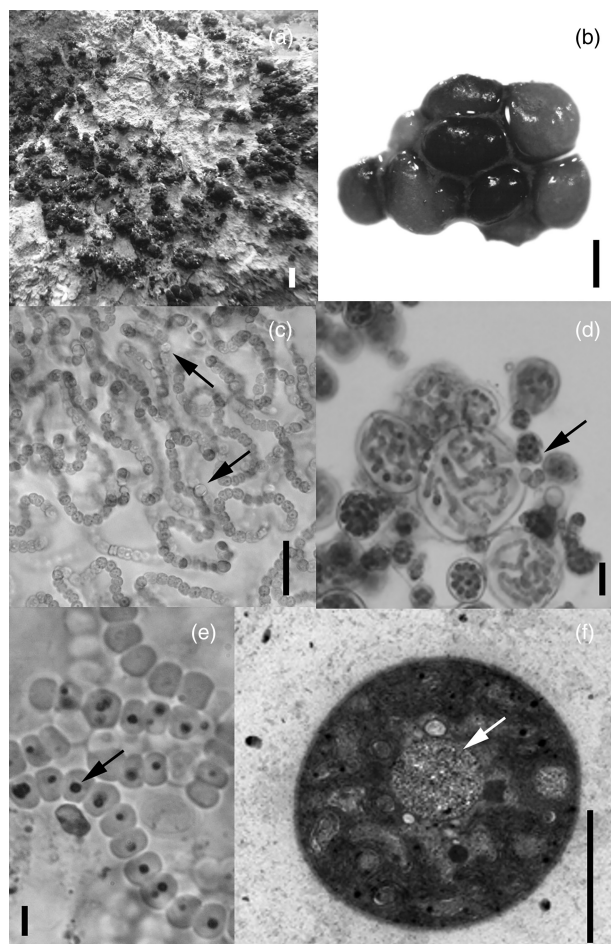


FIGURE 3 Micrographs of *Nostoc montejanii* under light microscopy: (a) habitat, (b) compact colonies, (c) filaments with internal and terminal heterocytes (arrows), (d) spherical young colonies, showing heterocytes appearing at the end of the colony (arrow), (e) one prominent polyphosphate granule by cell (arrow), (f) transmission electron microscope view, plain fascicular thylakoids and polyphosphate granule by cell (arrow). Scale bar: 1 cm for a and b; 30 µm for c and d; 3 µm for e and f.

($1528 \mu\text{S}\cdot\text{cm}^{-1}$), high DO ($8.4 \text{ mg}\cdot\text{L}^{-1}$), low nutrients (DIN $0.097 \text{ mg}\cdot\text{L}^{-1}$ and soluble reactive phosphorous 0.02), and high current velocity ($0.80 \text{ m}\cdot\text{s}^{-1}$).

Molecular and phylogenetic analyses

16S rRNA gene sequences

The 16S rRNA gene phylogenetic analysis showed our two species nested within the *Nostoc* sensu stricto cluster, which has a well-supported node (>97 MP/ML bootstrap and posterior probability values, Figure 2a,b). The clade pertaining to the *Nostoc* genus is formed by 22 clades, containing 19 morphospecies with well-supported nodes in most cases (>50 bootstrap values). Of note are the high support values ($\geq 99\%$ MP/ML bootstrap values and 100% posterior probability values) for the two species described herein (Figure 2b). In this tree,

Nostoc tlalocii is sister to *N. sphaericum* AB775902, with *N. montejanii* being the sister taxon to these two. While these clades (Figure 2b) show both high posterior probabilities values (≥ 91) and MP bootstrap (100%).

Percent identities based on the 16S rRNA gene sequence data were $>95\%$, the threshold typically considered as good evidence for identity in prokaryotes, and thus suggests that our species belong to *Nostoc* sensu stricto genus (Yarza et al., 2014). However, some species from other genera with similar morphologies to *Nostoc* were also $\leq 97\%$ identity with *Nostoc* sensu stricto species (Table 3). Considering that the threshold below 98% identity in prokaryotes serves as good evidence for separate species (Yarza et al., 2014), *Nostoc tlalocii* and *N. montejanii* showed $\geq 98\%$ identity both between each other and when compared with other *Nostoc* sensu stricto species, except with the species *N. edaphicum*, *N. carneum*, *N. desertorum*, and *N. indistinguendum* that showed $\leq 98\%$ (Table 2).

16S–23S ITS rRNA region

The phylogeny based on the 16S–23S ITS rRNA region provided better resolution for all species (Figure 5). In this analysis, *Nostoc tlalocii* was sister to *N. mirabile*, while *N. montejanii* was sister to the clade containing *N. tlalocii*, *N. mirabile*, *N. sphaeroides*, and *N. favosum*, with all nodes being well-supported. Several authors consider these phylogenetic analyses of this region to be useful for examining evolutionary relationships among species (Becerra-Absalón et al., 2020; González-Reséndiz et al., 2019; González-Reséndiz, Johansen, Alba-Lois, et al., 2018; González-Reséndiz, Johansen, Escobar-Sánchez, et al., 2018; Osorio-Santos et al., 2014), and the resulting tree provides further evidence to support the new species descriptions herein. Percent dissimilarities among 16S–23S ITS rRNA regions provide strong evidence that all species recognized in this study belong to different species (Becerra-Absalón et al., 2018, 2020; Bohunická et al., 2015; Erwin & Thacker, 2008; González-Reséndiz et al., 2019; González-Reséndiz, Johansen, Alba-Lois, et al., 2018; González-Reséndiz, Johansen, Escobar-Sánchez, et al., 2018; Hentschke et al., 2017; Osorio-Santos et al., 2014; Pietrasiak et al., 2014, 2019; Shalygin et al., 2017). All species in this comparison had $>3.0\%$ dissimilarity to all other species, indicating evolutionary lineages worthy of taxonomic recognition, while all clones of *Nostoc tlalocii* had $<1\%$ dissimilarity, indicating that these belong to the same species (Table 4). Our result for this analysis indicated that *N. montejanii* and *N. tlalocii* were different evolutionary lineages of the other species analyzed.

A final set of evidence for the recognition of both *Nostoc tlalocii* and *N. montejanii* lies in the comparisons

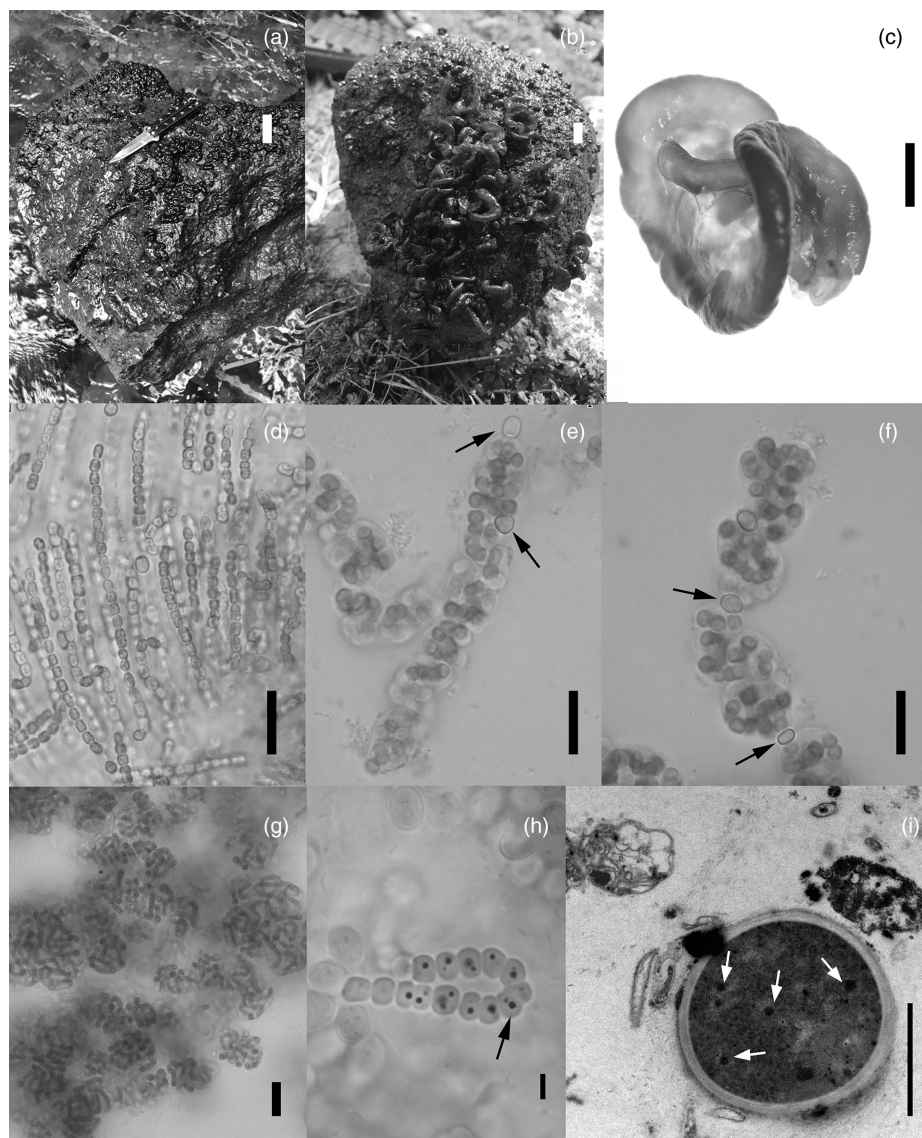


FIGURE 4 Micrographs of *Nostoc tlalocii* under light microscopy: (a–c) colonies spherical or ear-shaped in the habitat, (d) filaments with internal and terminal heterocytes, (e) multiseriate filaments, showing intercalary and apical heterocytes (arrows), (f) young colonies united by intercalary heterocytes (arrow), (g) juvenile colonies containing numerous uniseriate filaments, (h) several polyphosphate granules per cell (arrow), (i) transmission electron microscope view, plain fascicular thylakoids and several polyphosphate granule per cell (arrows). Scale bar: 1 cm for a–c; 30 μ m for d; 10 μ m for e–g; 3 μ m for h and i.

of the ITS rRNA region secondary structures. *Nostoc sensu stricto* has two distinct ribosomal operons, one with both tRNA genes and the other lacking tRNA genes; however, we did not have sequences of both operons for all study species (for example, we lacked the operon without tRNAs for *N. montejanii*). The most variable region of the D1-D1' helix was in the last stem portion and loop of the helix; *N. tlalocii* was quite dissimilar, with 5–20 distinct nucleotide substitutions from all other species, and *N. montejanii* differed considerably more, with 14–22 distinct nucleotide substitutions (Figure 6). Additionally, *N. montejanii* presented two unique mutations at position 31 and 44, both of which present a change from adenine to cytosine. These cytokines interact with guanines at positions 22 and 34,

breaking the structures of the two final loops characteristic of other *Nostoc* species. However, the basal part of secondary structure is very similar to the rest of the structures shown in Figure 6. The Box-B helices differed in the structure of the terminal loop, and the Box-B helix in *N. tlalocii* was the same in both operons. *Nostoc tlalocii* differed by 3–10 nucleotide substitutions from all other species, and *N. montejanii* differed even more with 6–12 nucleotide substitutions (Figure 7).

Finally, the V3 helices showed differences in length sequence and structure of the terminal loop in all species of the genus. *Nostoc tlalocii* had 10–19 distinct nucleotide substitutions compared with all other species, while *N. montejanii* had 8–21 distinct nucleotide substitutions (Figure 8).

TABLE 3 Percent similarity of strains based on *p*-distance analysis of the 16S rRNA gene sequence data; percent similarity = $100 \times (1 - p)$.

	1	2	3	4	5	6	7	8	9	10	11	12	13	14	15	16	17
1. <i>Nostoc montejanii</i> clone 46.33	—																
2. <i>Nostoc flabocli</i> clone 32.3	98	—															
3. <i>Nostoc sphaericum</i> AB775902	99	98	—														
4. <i>Nostoc favosum</i> NZ_JAIVFQ010000206	98	98	99	—													
5. <i>Nostoc mirabile</i> MW649142	98	98	98	98	—												
6. <i>Nostoc edaphicum</i> HQ700837	98	97	98	98	98	—											
7. <i>Nostoc calcicola</i> AJ630447	98	98	98	98	98	99	—										
8. <i>Nostoc carneum</i> JQ07	97	97	98	98	98	100	100	—									
9. <i>Nostoc commune</i> AY577536	98	98	99	98	97	98	99	98	—								
10. <i>Nostoc desertorum</i> AY577537	96	96	97	96	96	97	97	97	98	—							
11. <i>Nostoc indistinguishendum</i> AY577538	97	98	98	97	96	97	98	98	98	97	—						
12. <i>Nostoc lichenoides</i> AY577535	98	98	98	98	97	99	99	99	98	98	97	—					
13. <i>Nostoc neudorfense</i> MK300544	98	98	98	98	98	99	99	99	99	97	98	99	—				
14. <i>Nostoc piscinale</i> JQ070067	98	98	99	98	98	98	98	98	99	96	98	98	99	—			
15. <i>Nostoc</i> sp. EU022707	98	98	98	98	98	99	100	99	99	97	98	98	99	98	—		
16. <i>Nostoc punctiforme</i> NR074317	98	98	99	98	97	99	99	99	99	98	98	99	100	98	99	—	
17. <i>Nostoc verrucosum</i>	98	98	98	98	97	98	99	99	99	97	98	99	99	98	99	99	—
18. <i>Violetonostoc minutum</i> MN400069	95	96	95	95	95	95	96	95	95	95	95	95	95	95	96	95	95
19. <i>Roholtiella edaphica</i> KM268878	96	97	96	96	96	97	97	97	96	96	96	96	97	96	97	96	96
20. <i>Purpureonostoc tibetica</i> MN381942	94	95	94	94	94	94	94	94	94	93	94	94	94	94	95	94	94
21. <i>Pseudolaiinostoc soli</i> MH497065	95	95	94	94	94	95	95	94	94	93	94	94	94	93	95	94	93
22. <i>Parakomarekiella sesnandensis</i> MT044190	95	96	96	95	95	96	97	96	96	95	96	95	96	95	96	96	95
23. <i>Mojavia pulchra</i> AY577534	95	96	95	95	95	96	96	96	96	95	96	96	96	95	96	96	95
24. <i>Komarekiella atlantica</i> KX638487	96	97	96	96	96	97	97	97	96	96	96	96	96	96	97	96	96
25. <i>Halotia branconii</i> KJ843310	95	95	95	95	95	95	95	94	94	94	94	95	95	94	95	95	94
26. <i>Compactonostoc shennongjiaensis</i> MH598843	95	96	95	95	95	97	97	97	96	96	96	96	96	96	97	96	96
27. <i>Atlanticothrix silvestris</i> NR172568	95	96	96	95	95	95	96	95	95	95	96	95	96	95	96	96	95
28. <i>Amazonocrinis nigriferae</i> NR_172622	96	95	96	95	95	96	97	96	96	95	95	96	96	96	97	96	96
29. <i>Aliinostoc morphoplasticum</i> KY403996	94	94	94	94	93	93	93	93	93	92	93	93	93	93	94	93	93
30. <i>Desikacharya nostocoides</i> MH036167	94	94	94	94	93	94	95	95	95	93	94	95	95	94	95	95	95
31. <i>Desmonostoc muscorum</i> AM711524	97	97	97	96	97	97	97	97	96	95	95	97	97	97	97	96	97

Note: Comparisons between *Nostoc* species are in black bold font. Comparisons of *Nostoc* species with other genera are in gray bold font.

Morphological analysis

The morphological comparison among our populations showed important differences in populations from two different geographic areas (Tambaque River and Mexico valley streams). The colony color in *Nostoc montejanii* is black, while in *N. tlalocii*, it is brown. The length and width of cells were greater in *N. montejanii* (3.1–5 µm long and 4–6.1 µm wide) than in *N. tlalocii* (1.5–4.2 µm long and 3.2–4.6 µm wide). Furthermore, *N. tlalocii* presented more polyphosphate granules in its cells (up to four small granules per cell) than in *N. montejanii* (one prominent granule per cell). *Nostoc montejanii* also formed a distinctive life cycle phase, a seriated filaments, that was not seen in *N. tlalocii*.

Morphological comparisons were also made between our populations and *Nostoc* species that live in similar environments, in this case, streams (Table 2).

The thallus characteristic differed between the six species analyzed in its form, color, and size of colonies (Table 2, Figures 3 and 4).

Regarding the size of the cells (Table 2), *Nostoc montejanii* was similar to *N. verrucosum* with cells that overlapped within the range of 3–5 µm long and 6–6.1 µm wide; however, *N. montejanii* presented slightly smaller cells than *N. verrucosum* (≤5 µm long and ≤6 µm wide vs. up to 6 µm long and 6 µm wide, respectively). While *N. tlalocii* showed similar cell sizes as *N. parmelioides* given their overlapping ranges of 2–5 µm length and 3.5–4.2 µm width, shorter cells were observed in *N. tlalocii* than *N. parmelioides* (1.4–1.8 µm vs. ≥2.2 µm, respectively), and *N. parmelioides* had wider cells than *N. tlalocii* (up to 5.2 µm vs. ≤4.2 µm, respectively).

Regarding the heterocytes of the distinct species, *Nostoc montejanii*, *N. tlalocii*, and *N. letestui* had spherical heterocytes, while those of *N. parmelioides* and *N. membranaceus* were oval-shaped. In size, *N. letestui* had the biggest heterocytes with 10 µm diameter, while *N. montejanii* and *N. tlalocii* overlapped inside the range of 3.2–4.6 µm, with those of *N. montejanii* being slightly larger reaching up to 5.2 µm.

DISCUSSION

Nostoc sensu stricto is a monophyletic taxon diagnosable from the other members of Nostocaceae. In all phylogenetic analyses, the *Nostoc sensu stricto* clade was strongly supported as monophyletic, being sister to the *Mojavia* genus, a relationship with strong support in the BI, ML, and MP analyses (Figure 2a). The two species analyzed herein are nested inside the *Nostoc sensu stricto* clade (Figure 2b), and their heterocyte and vegetative filament morphologies, as well as life cycles, are consistent with *Nostoc* species characteristics (Komárek, 2013). According to Yarza et al. (2014), percent identity greater than 95%

serves as good evidence for species belonging to same genus; however, some species of other genera showed >95% identities with *Nostoc sensu stricto* species, suggesting that this criteria is not as strong within the Nostocales. Previous studies have demonstrated that Nostocales are highly similar in their 16S rRNA gene sequences (Flechtner et al., 2002; Kaštovský et al., 2014; Lukešová et al., 2009) and that genera in this order frequently show similarities greater than 98% with other genera. In response, Kaštovský et al. (2014) proposed discriminating between species and genera within Nostocales using the <99% and <98% similarity thresholds, respectively, at the 16S rRNA gene. The *p*-distance analysis (Table 3) showed equal or greater than 98% similarity between species of *Nostoc sensu stricto* in most cases, including our species, according to Kaštovský et al. (2014). Only five species (*N. mirabile*, *N. edaphicum*, *N. carneum*, *N. desertorum*, and *N. indistinctum*) showed 97% similarity with several other *Nostoc sensu stricto* species.

The phylogenetic tree of the 16S–23S ITS rRNA region recovered the two studied populations in separate clades with different sister taxa, giving further evidence that they comprise distinct species (Figure 5). We also analyzed the secondary structures of the 16S–23S ITS rRNA region, which was recently suggested as a useful character for genus-level taxonomy (Becerra-Absalón et al., 2018, 2020; Boyer et al., 2001; Hentschke et al., 2017; Johansen & Casamatta, 2005; Osorio-Santos et al., 2014; Siegesmund et al., 2008). The conserved domains in the 16S–23S ITS rRNA region and structures of the D1–D1', Box-B, and V3 helices in *Nostoc sensu stricto*, including the Mexican species studied herein, were strong evidence for congeneric assignment, but in all regions were different indicating *N. tlalocii* and *N. montejanii* were different species (Figures 6–8). The high sequence dissimilarity of the ITS rRNA region between homologous operons of the two Mexican species provides additional molecular evidence for species recognition. As a general rule, strains/sequences within the same species tend to have percent dissimilarities averaging ~1.0% and pairwise comparisons less than ~3.0%, while different species tend to have percent dissimilarities >4.0% and demonstrate reciprocal monophyly (Erwin & Thacker, 2008). The two Mexican species in this study had percent dissimilarities of >10.5% in the operons with both tRNA genes (Table 4). Several authors have declared >7.0% between different populations to be strong evidence for separate species (Becerra-Absalón et al., 2018, 2020; González-Reséndiz, Johansen, Alba-Lois, et al., 2018; Hentschke et al., 2017; Osorio-Santos et al., 2014; Pietrasiak et al., 2014; Shalygin et al., 2017). Furthermore, all sequences belonging to *N. tlalocii* had <0.7% dissimilarities, confirming their shared specific identity as per the rule proposed by Erwin and Thacker (2008).

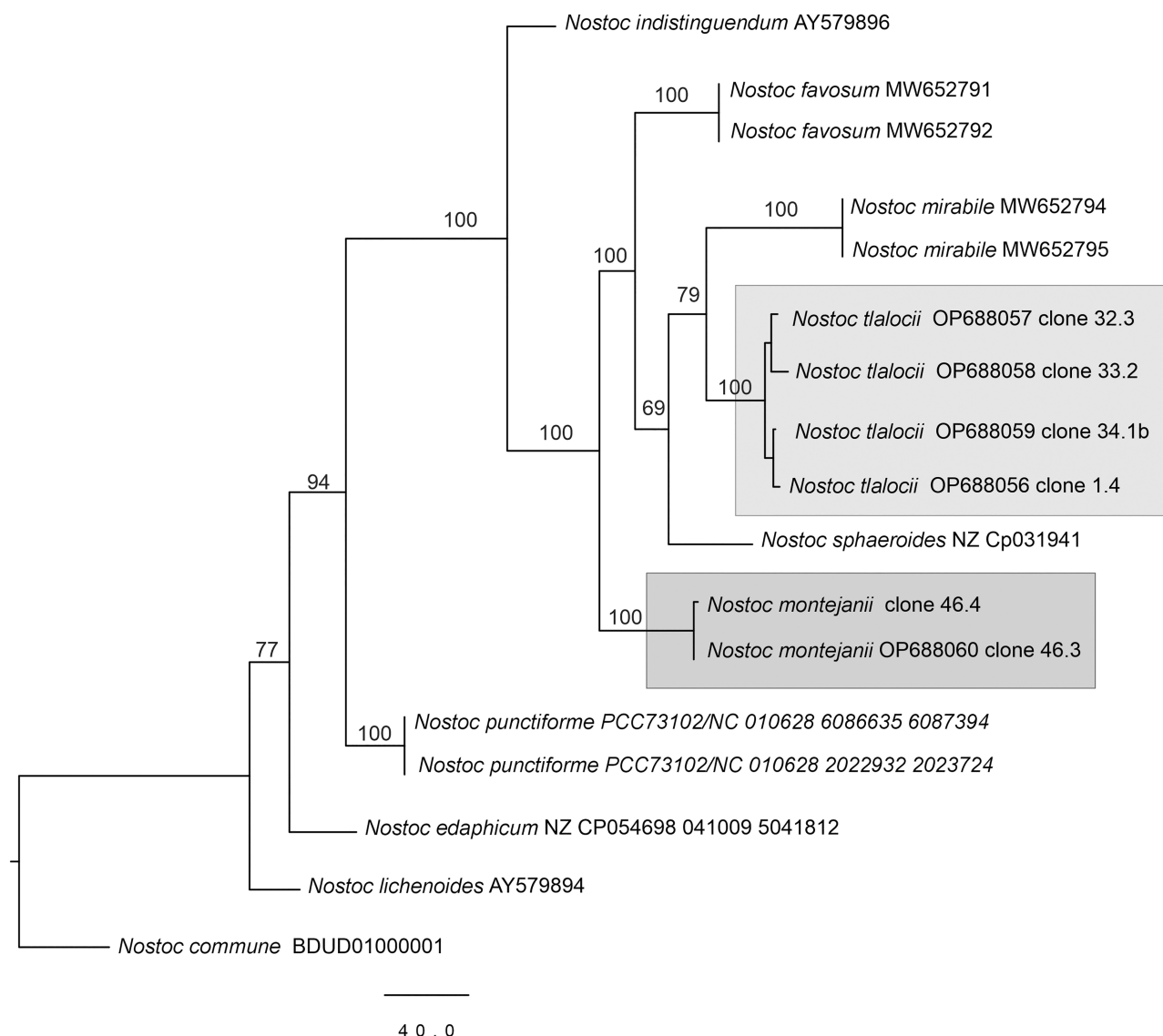


FIGURE 5 Maxima Parsimony analysis of 14 *Nostoc* sensu stricto OTUs, based on a 700-nucleotide alignment of 16S–23S ITS rRNA region, with bootstrap values mapped onto nodes. In light gray square: *N. tlalocii*; dark gray square: *N. montejanii*.

The populations from the two different geographic areas in Mexico showed some morphological differences (Table 2), such as colony color (black in *Nostoc montejanii* and brown in *N. tlalocii*) and larger cell size in *N. montejanii* than *N. tlalocii* (3.1–5.2 μm long and 4–6.1 μm wide vs. 1.5–4.2 μm long and 3.2–4.6 μm wide, respectively). *Nostoc tlalocii* presented more polyphosphate granules (up to four small granules per cell) in its cells than observed in *N. montejanii* (one prominent granule per cell), and *N. montejanii* formed a distinctive life cycle phase, aseriated filaments, that was not seen in *N. tlalocii*.

The comparison between the studied Mexican populations with others *Nostoc* species showed that *N. montejanii* is similar to *N. verrucosum*, but they differ in color (black in *N. montejanii* and olive green to dark brown in *N. verrucosum*), thallus height (1.2–2 cm in *N. montejanii* and 5–10 cm in *N. verrucosum*), cell size

(smaller cells in *N. montejanii* $\leq 5 \mu\text{m}$ long and $\leq 6 \mu\text{m}$ wide vs. larger cells in *N. verrucosum* up to 6 μm long and 6 μm wide), and heterocyte form and size, with those in *N. montejanii* being spherical (3.3–5.2 μm in diameter) and those in *N. verrucosum* being oval (7 μm long and 5 μm wide).

Nostoc tlalocii is similar to *N. parmelioides* but differed by having larger colonies (up to 4.6 cm height vs. 2 cm in *N. parmelioides*), shorter cells ($\leq 1.8 \mu\text{m}$ length vs. $\geq 2.2 \mu\text{m}$ in *N. parmelioides*), and spherical and shorter heterocytes ($\leq 4.6 \mu\text{m}$ diameter vs. oval heterocytes $\geq 4.8 \mu\text{m}$ in *N. parmelioides*).

Finally, the ecological preferences of the two species can be distinguished by their exclusive habitats of lotic environments, their geological origin, and their different tolerance to nutrients (Table 1). On the one hand, *Nostoc montejanii* clearly inhabits high-current and oligotrophic rivers in coastal plain regions of calcareous

TABLE 4 Mean percent dissimilarities based on a sequence alignment of the 16S–23S ITS rRNA region.

	1	2	3	4	5	6	7	8	9	10	11	12	13
1. <i>Nostoc montejanii</i> clone 46.3	—												
2. <i>Nostoc montejanii</i> clone 46.4	0.3	—											
3. <i>Nostoc tlalocii</i> clone 1.4	15.1	15.4	—										
4. <i>Nostoc tlalocii</i> clone 32.3	15.1	15.5	0.5	—									
5. <i>Nostoc tlalocii</i> clone 33.2	15.5	15.8	0.9	0.3	—								
6. <i>Nostoc tlalocii</i> clone 34.1	14.4	15.0	0.5	0.3	0.7	—							
7. <i>Nostoc mirabile</i> MW652794	12.3	12.7	10.4	10.5	10.9	10.4	—						
8. <i>Nostoc sphaeroides</i> NZCP031941	12.6	12.9	11.5	11.7	12.0	11.0	11.5	—					
9. <i>Nostoc favosum</i> MW652791	14.1	14.5	12.3	12.6	12.9	12.0	12.7	12.2	—				
10. <i>Nostoc edaphicum</i> NZCP054698	14.4	14.8	12.5	13.0	13.4	12.0	11.9	11.7	14.3	—			
11. <i>Nostoc indistinguishendum</i> AY579896	14.5	14.9	14.1	14.6	14.9	13.6	13.0	13.0	11.1	7.0	—		
12. <i>Nostoc lichenoides</i> AY579894	16.7	17.1	12.9	13.4	13.8	12.7	14.6	13.0	13.9	9.0	9.1	—	
13. <i>Nostoc punctiforme</i> PCC73102	14.1	14.5	13.8	14.2	14.5	13.5	14.9	12.0	12.5	9.2	8.2	9.6	—
14. <i>Nostoc commune</i> BDUD01000001	18.2	18.5	15.3	15.7	16.1	14.5	15.2	14.0	16.9	13.1	14.8	12.6	13.2

Note: Values >7.0 are considered strong evidence that compared groups belong to different species, values >3.0 are likely different species, while values ~1.0 (in bold), likely indicate compared groups belong to the same species (Erwin & Thacker, 2008; González-Reséndiz et al., 2019; Osorio-Santos et al., 2014; Pietrasiak et al., 2014, 2019).

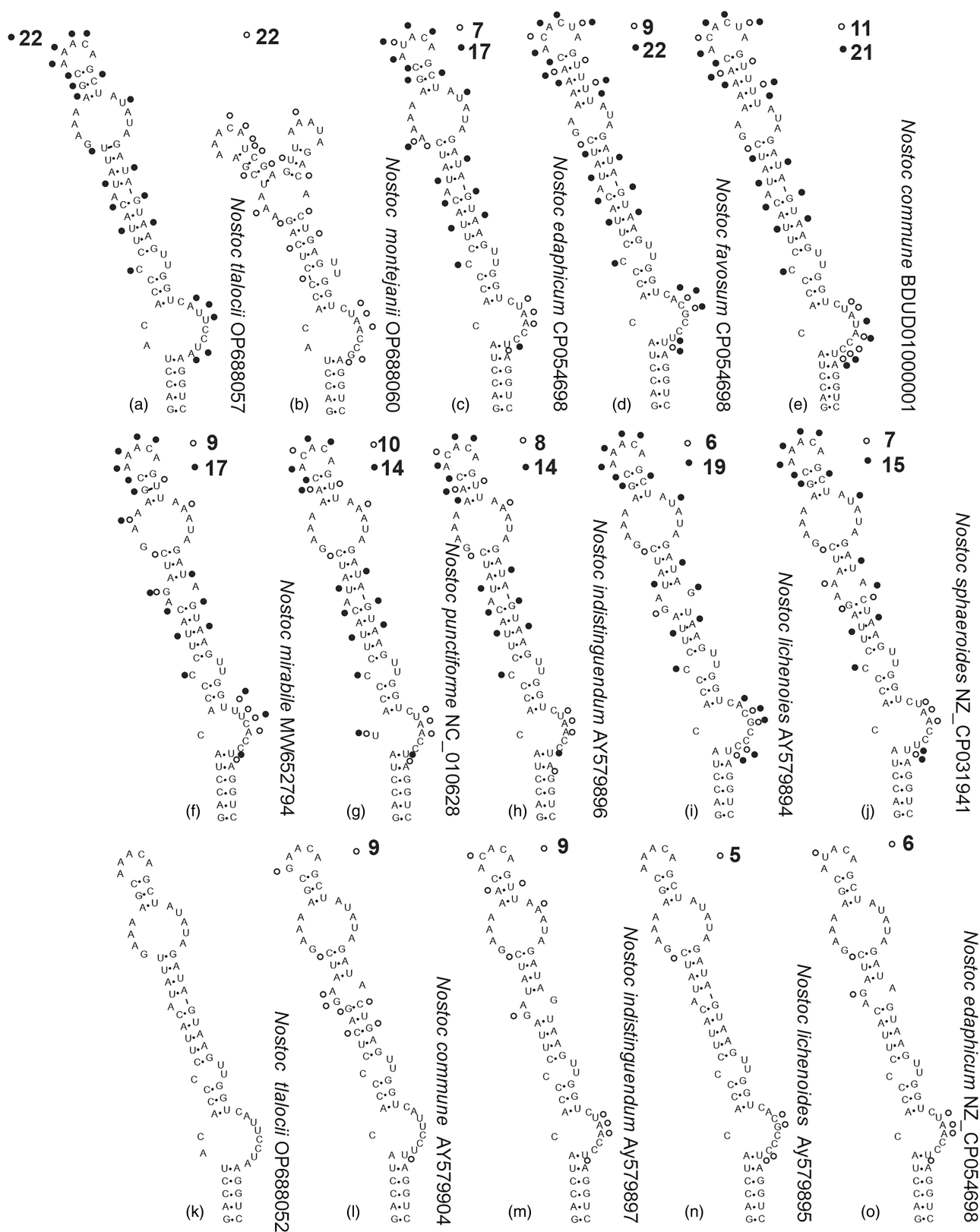


FIGURE 6 Secondary structure of the D1-D1' helix in *Nostoc sensu stricto* species, with nucleotides differing from *N. tlaocii* due to substitutions, insertions, or deletions marked with open circles, and nucleotides similarly differing from *N. montejanii* marked with solid circles; summary numbers of nucleotide differences given above each helix.

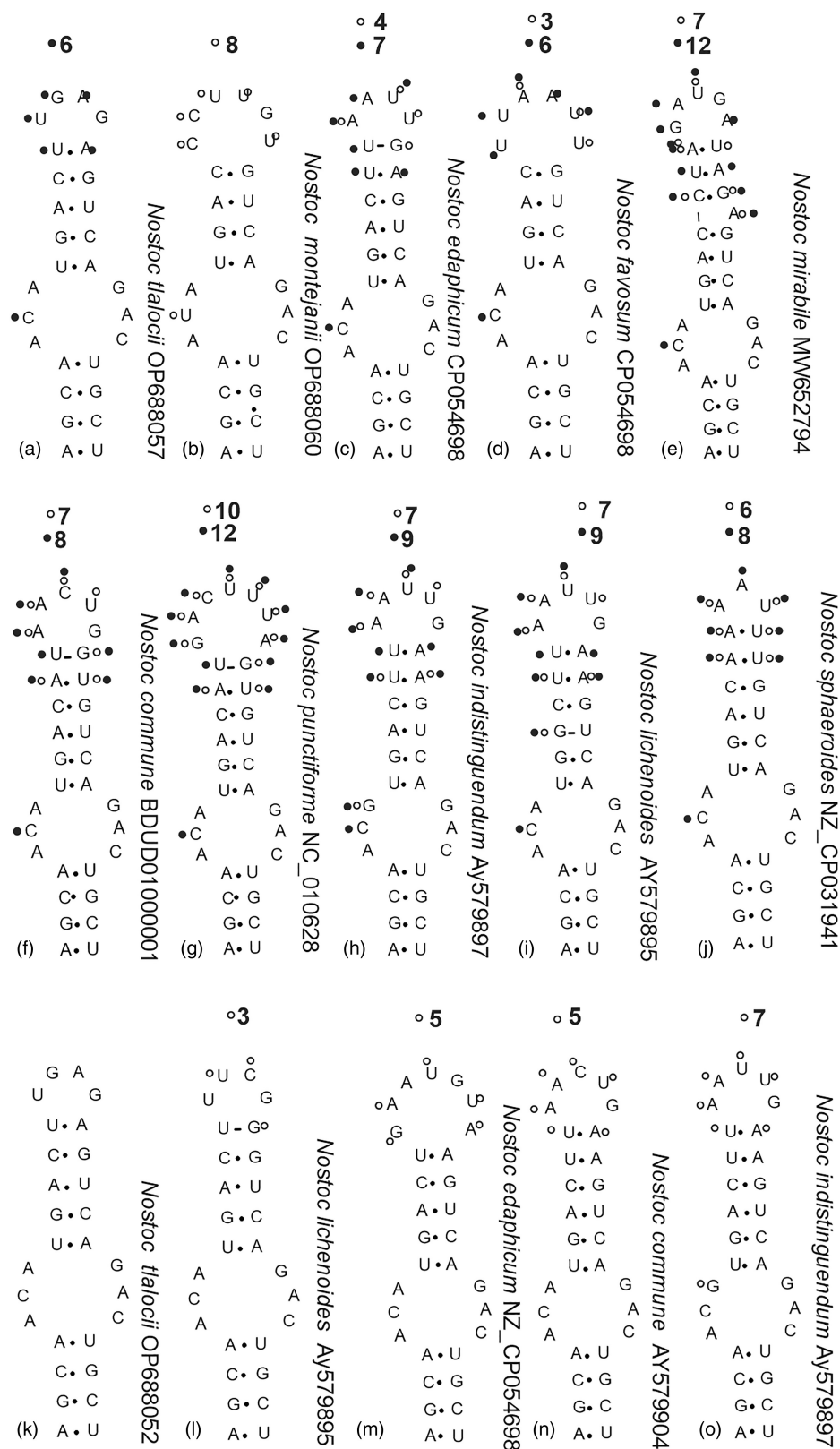


FIGURE 7 Secondary structure of the Box-B helix in *Nostoc* sensu stricto species, with nucleotides differing from *N. tlaocii* due to substitutions, insertions, or deletions marked with open circles, and nucleotides similarly differing from *N. montejanii* marked with solid circles; summary numbers of nucleotide differences given above each helix.

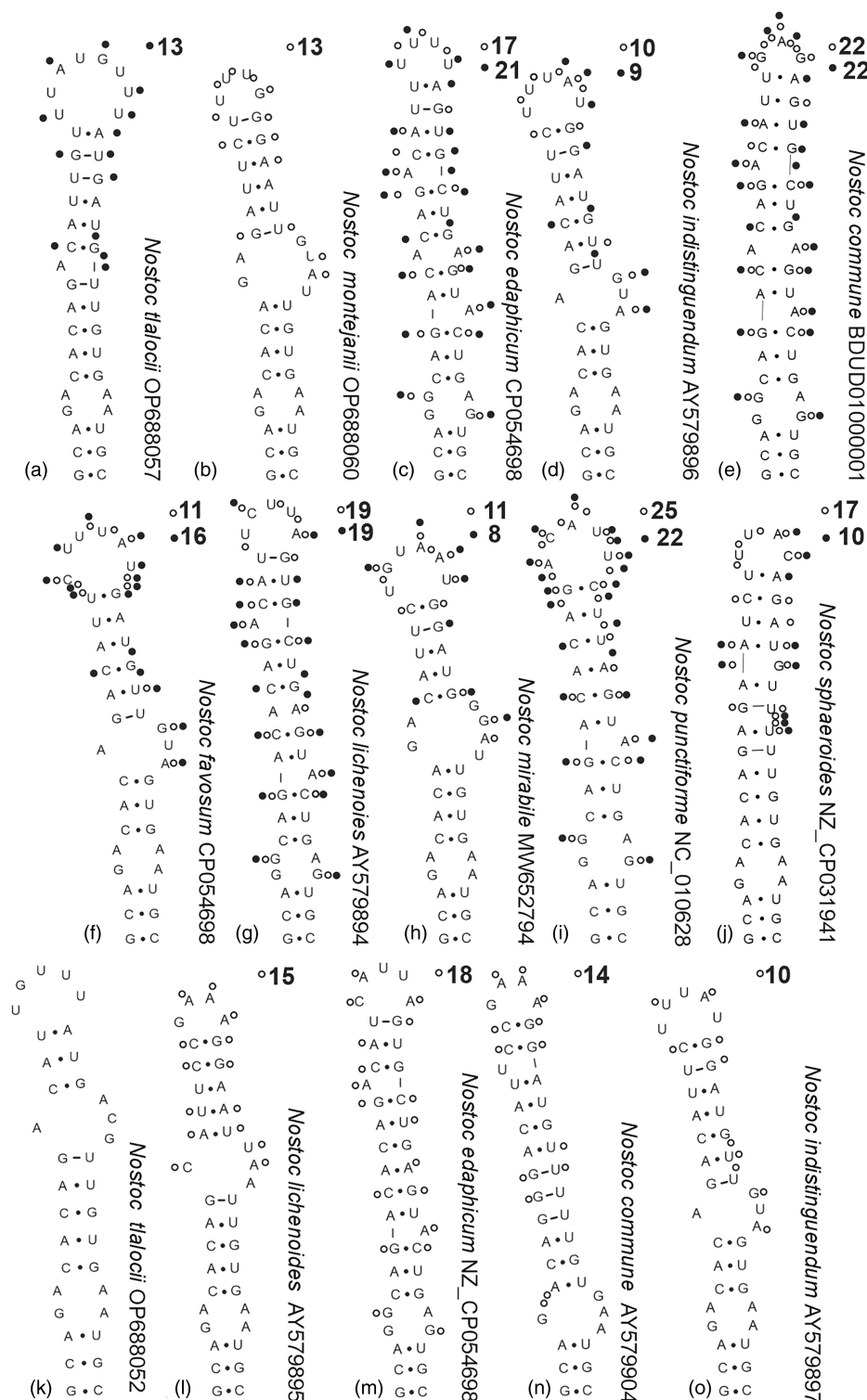


FIGURE 8 Secondary structure of the V3 helix in *Nostoc sensu stricto* species, with nucleotides differing from *N. tlaocii* due to substitutions, insertions, or deletions marked with open circles, and nucleotides similarly differing from *N. montejanii* marked with solid circles; summary numbers of nucleotide differences given above each helix.

geological origin. On the other hand, *N. tlaocii* grows in siliceous geological regions and is also tolerant to the presence of higher concentrations of DIN and soluble reactive phosphorous.

Together with *Nostoc verrucosum* and *N. pamelioides*, the populations of *N. montejanii* and *N. tlaocii* form a group with a preference for inhabiting lotic environments (Dodds & Marra, 1989; Sabater & Muñoz, 2000).

The high current speed recorded in the rainy season and the lower temperatures of both geographical regions in Mexico seem to be related to the greater abundance and more compact growths (compact and ear-shaped colonies) in which they are found (Carmona-Jiménez et al., 2022). The interaction between the ear-shaped *Nostoc* populations and Chironomidae larvae has been described in other *Nostoc* species such as *N. parmelioides* (Dodds & Marra, 1989) and *N. verrucosum* (Sabater & Muñoz, 2000), suggesting that this is not an isolated interaction and that it may be an evolutionary convergence that is registered in different geographical regions in the world. In these instances, chironomids seek refuge and modify the form of each colony to be ear-shaped in areas of high current and use the algae as a source of nutrients during its larval stages of development until hatching into the aerial phase. Based on the combined morphological, ecological, and molecular evidence, we conclude that the populations from two different geographic areas constitute different species, and we describe the Mexican populations as new species.

AUTHOR CONTRIBUTIONS

Javier Carmona Jiménez: Conceptualization (lead); formal analysis (equal); funding acquisition (equal); investigation (lead); methodology (equal); resources (equal); writing – original draft (equal); writing – review and editing (equal). **Angela Caro Borrero:** Conceptualization (equal); data curation (equal); formal analysis (equal); investigation (equal); methodology (equal); writing – original draft (equal). **Itzel Becerra-Absalón:** Formal analysis (equal); investigation (equal); methodology (equal); writing – original draft (equal); writing – review and editing (equal). **Elvira Perona Urizar:** Conceptualization (equal); formal analysis (equal); funding acquisition (equal); investigation (equal); methodology (equal). **Kenia Márquez Santamaría:** Data curation (equal); formal analysis (equal); investigation (equal); methodology (equal). **Pilar Mateo Ortega:** Conceptualization (equal); formal analysis (equal); funding acquisition (equal); investigation (equal); methodology (equal); writing – review and editing (equal).

ACKNOWLEDGMENTS

We thank the Dirección de Asuntos del Personal Académico (DGAPA) at UNAM for supporting the PAPIIT Projects IN307219 and IN206821 and CIANOPARK (OAPN 2593/2020), Ministerio Español para la Transición Ecológica y Reto Demográfico for supporting genetic analysis. We also thank María Eugenia Muñiz Díaz de León for technical assistance in gene quantification, Ricardo García Sandoval for technical assistance in imaging the secondary structure of ITS, and Edgar Caro Borrero for the map drawing. Brett O. Butler provided English style and grammar corrections for the manuscript.

ORCID

Javier Carmona Jiménez  <https://orcid.org/0000-0003-0420-4863>
 Angela Caro Borrero  <https://orcid.org/0000-0001-7352-5447>
 Itzel Becerra-Absalón  <https://orcid.org/0000-0002-4071-541X>
 Elvira Perona Urizar  <https://orcid.org/0000-0001-8761-6702>
 Kenia Márquez Santamaría  <https://orcid.org/0000-0002-6474-4004>
 Pilar Mateo Ortega  <https://orcid.org/0000-0003-1351-269X>

REFERENCES

- American Public Health Association. (1995). *Standard methods for the examination of water and wastewater* (19th ed.). American Public Health Association.
- Bagchi, S. N., Dubey, N., & Singh, P. (2017). Phylogenetically distant clade of *Nostoc*-like taxa with the description of *Aliinostoc* gen. nov. and *Aliinostoc morphoplaticum* sp. nov. *International Journal of Systematic and Evolutionary Microbiology*, 67(9), 3329–3338.
- Becerra-Absalón, I., Johansen, J. R., Muñoz-Martín, M., & Montejano, G. (2018). *Chroakolemma* gen. nov. (Leptolyngbyaceae, cyanobacteria) from soil biocrusts in the semi-desert central region of Mexico. *Phytotaxa*, 367, 201–218.
- Becerra-Absalón, I., Johansen, J. R., Osorio-Santos, K., & Montejano, G. (2020). Two new *Oculatella* (Oculatellaceae, Cyanobacteria) species in soil crusts from tropical semi-arid uplands of Mexico. *Fottea*, 20(2), 160–170.
- Bertani, G. (1951). Studies on lysogenesis. I. The mode of phage liberation by lysogenic *Escherichia coli*. *Journal of Bacteriology*, 62(3), 293–300.
- Bohunická, M., Pietrasiak, N., Johansen, J. R., Berrendero, E., Hauer, T., Gaysina, L. A., & Lukešová, A. (2015). *Roholtia* gen. nov. (Nostocales, cyanobacteria) – A tape-ring and branching cyanobacteria of the family Nostocaceae. *Phytotaxa*, 197, 84–103.
- Boyer, S., Flechtner, V., & Johansen, J. R. (2001). Is the 16S-23S rRNA internal transcribed spacer region a good tool for use in molecular systematics and population genetics? A case study in cyanobacteria. *Molecular Biology and Evolution*, 18, 1057–1069. <https://doi.org/10.1093/oxfordjournals.molbev.a003877>
- Cai, F., & Li, R. (2020). *Purpleonostoc*, a new name for a recently described genus of *Nostoc*-like cyanobacteria. *Fottea, Olomouc*, 20(2), 111.
- Cai, F., Li, X., Geng, R., Peng, X., & Li, R. (2019). Phylogenetically distant clade of *Nostoc*-like taxa with the description of *Minunostoc* gen. nov. and *Minunostoc cylindricum* sp. nov. *Fottea, Olomouc*, 19(1), 13–24.
- Cai, F., Li, X., Yang, Y., Jia, N., Huo, D., & Li, R. (2019). *Compactonostoc shennongjiaensis* gen. & sp. nov. (Nostocales, Cyanobacteria) from a wet rocky wall in China. *Phycologia*, 58(2), 200–210.
- Cai, F., Peng, X., & Li, R. (2020). *Violetonostoc minutum* gen. et sp. nov. (Nostocales, Cyanobacteria) from a rocky substrate in China. *Algae*, 35(1), 1–15.
- Cai, F., Yu, G., Liu, Y., Sun, Y., & Li, R. (2021). Description of two new species of *Nostoc* from China based on the polyphasic approach. *Fottea*, 21(2), 259–271.
- Carmona-Jiménez, J., Salinas-Camarillo, V., & Caro-Borrero, A. (2022). The Macroalgae Ecological Quality Index (MEQI) in the basin of Mexico: A proposal of aquatic bioindicators for peri-urban rivers. *Revista Mexicana de Biodiversidad*, 93(1), e933899. <https://doi.org/10.22201/ib.20078706e.2022.93.3899>

- Cartajena, A. M., Carmona-Jiménez, J., & Perona, U. E. (2020). Aspectos ecológicos, taxonómicos y de distribución de cianobacterias bentónicas en cinco ríos de la región central de México [Ecological, taxonomic and distribution aspects of benthic cyanobacteria in five rivers of the central region of Mexico]. *Acta Botánica Mexicana*, 127, e1639. <https://doi.org/10.21829/abm127.2020.1639>
- Dodds, W. K., Gudder, D. A., & Mollenhauer, D. (1995). The ecology of *Nostoc*. *Journal of Phycology*, 31(1), 2–18.
- Dodds, W. K., & Marra, J. L. (1989). Behaviors of the midge, *Cricotopus* (Diptera, Chironomidae) related to mutualism with *Nostoc parmelioideus* (Cyanobacteria). *Aquatic Insects*, 11(4), 201–208.
- Drummond, A. J., Ho, S. Y. W., Philips, M. J., & Rambaut, A. (2006). Relaxed phylogenetics and dating with confidence. *PLoS Biology*, 4, e88.
- Erwin, P. M., & Thacker, R. W. (2008). Cryptic diversity of the symbiotic cyanobacterium *Synechococcus spongiarum* among sponge hosts. *Molecular Ecology*, 17, 2937–2947. <https://doi.org/10.1111/j.1365-294X.2008.03808.x>
- Flehtner, V. R., Boyer, S. L., Johansen, J. R., & Denoble, M. L. (2002). *Spirirestis rafaensis* gen. et sp. nov. (Cyanophyceae), a new cyanobacterial genus from arid soils. *Nova Hedwigia*, 74, 1–24.
- Gelman, A., & Rubin, D. B. (1992). Inference from iterative simulation using multiple sequences. *Statistical Science*, 7, 457–472.
- Genuário, D. B., Vaz, M. G. M. V., Hentschke, G. S., Sant'Anna, C. L., & Fiore, M. F. (2015). *Halotia* gen. nov., a phylogenetically and physiologically coherent cyanobacterial genus isolated from marine coastal environments. *International Journal of Systematic and Evolutionary Microbiology*, 65, 663–675.
- González-Reséndiz, L., Johansen, J., Alba-Lois, L., Segal-Kischinevsky, C., Escobar-Sánchez, V., Jiménez-García, L. F., Hauer, T., & León-Tejera, H. (2018). *Nunduva*, a new marine genus of Rivulariaceae (Nostocales, cyanobacteria) from marine rocky shores. *Fottea*, 18, 86–105.
- González-Reséndiz, L., Johansen, J., Escobar-Sánchez, V., Segal-Kischinevsky, C., Jiménez García, L. F., & León-Tejera, H. (2018). Two new species of *Phyllonema* (Rivulariaceae, Cyanobacteria) with an emendation of the genus. *Journal of Phycology*, 54, 638–652.
- González-Reséndiz, L., Johansen, J. R., León-Tejera, H., Sanchez, L., Segal-Kischinevsky, C., Escobar-Sánchez, V., & Morales, M. (2019). A bridge too far in naming species: A total evidence approach does not support recognition of four species in *Desertifilum* (cyanobacteria). *Journal of Phycology*, 55, 898–911.
- Guiry, M. D., & Guiry, G. M. (2023). *AlgaeBase*. World-Wide Electronic Publication, National University of Ireland, Galway. <https://www.algaebase.org>
- Hall, T. A. (1999). BioEdit: A user-friendly biological sequence alignment editor and analysis program for Windows 95/98/NT. *Nucleic Acids Symposium Series*, 41, 95–98.
- Hentschke, G. S., Johansen, J. R., Pietrasiak, N., Rigonato, J., Fiore, M. F., & Sant'Anna, C. L. (2017). *Komarekiella atlantica* gen. et sp. nov. (Nostocaceae, Cyanobacteria): A new subaerial taxon from the Atlantic rainforest and Kauai, Hawaii. *Fottea*, 17(2), 178–190.
- Holmgren, P. K., Holmgren, N. H., & Barnett, L. C. (1990). *Regnum vegetabile. Vol. 120: Index herbariorum. Part I. The herbaria of the world* (8th ed.). New York Botanical Gardens.
- Hrouzek, P., Lukešová, A., Mareš, J., & Ventura, S. (2013). Description of the cyanobacterial genus *Desmonostoc* gen. nov. including *D. muscorum* comb. nov. as a distinct, phylogenetically coherent taxon related to the genus *Nostoc*. *Fottea*, 13(2), 201–213.
- Johansen, J. R., & Casamatta, D. A. (2005). Recognizing cyanobacterial diversity through adoption of a new species paradigm. *Algological Studies*, 117(1), 71–93.
- Kaštovský, J., Berrendero-Gomez, E., Hladil, J., & Johansen, J. R. (2014). *Cyanocohniella calida* gen. nov. et spec. nov. (Cyanobacteria: Aphanizomenonaceae) a new cyanobacterium from the thermal springs from Karlovy Vary, Czech Republic. *Phytotaxa*, 181, 279–292.
- Komárek, J. (2006). Cyanobacterial taxonomy: Current problems and prospects for the integration of traditional and molecular approaches. *Algae*, 21, 349–375.
- Komárek, J. (2013). *Cyanoprokaryota. Part 3: Heterocytous genera*. Springer Spektrum.
- Komárek, J., Kaštovský, J. M., & Johansen, J. R. (2014). Taxonomic classification of cyanoprokaryotes (cyanobacterial genera) 2014, using a polyphasic approach. *Preslia*, 86, 295–335.
- Kumar, S., Stecher, G., & Tamura, K. (2016). MEGA7: Molecular evolutionary genetics analysis version 7.0 for bigger datasets. *Molecular Biology and Evolution*, 33, 1870–1874.
- Lee, N. J., Bang, S. D., Kim, T., Ki, J. S., & Lee, O. M. (2021). *Pseudoallinostoc sejongensis* gen. & sp. nov. (Nostocales, Cyanobacteria) from floodplain soil of the Geum River in Korea based on polyphasic approach. *Phytotaxa*, 479(1), 55–70.
- Lepère, C., Wilmette, A., & Meyer, B. (2000). Molecular diversity of *Microcystis* strains (Cyanophyceae, Chroococcales) based on 16S rDNA sequences. *Systematics and Geography of Plants*, 70, 27–283.
- Lukešová, A., Johansen, J. R., Martin, M. P., & Casamatta, D. (2009). *Aulosira bohemosensis* sp. nov.: Further phylogenetic uncertainty at the base of the Nostocales (Cyanobacteria). *Phycologia*, 48, 118–129.
- Mateo, P., Douterelo, I., Berrendero, E., & Perona, E. (2006). Physiological differences between two species of cyanobacteria in relation to phosphorus limitation. *Journal of Phycology*, 42, 61–66.
- Mateo, P., Perona, E., Berrendero, E., Leganés, F., Martín, M., & Golubia, S. (2011). Life cycle as a stable trait in the evaluation of diversity of *Nostoc* from biofilms in rivers. *FEMS Microbiology Ecology*, 76, 185–198.
- Mesfin, M., Johansen, J. R., Pietrasiak, N., & Baldarelli, L. M. (2020). *Nostoc oromo* sp. nov. (Nostocales, cyanophyceae) from Ethiopia: A new species based on morphological and molecular evidence. *Phytotaxa*, 433(2), 81–93.
- Mollenhauer, D. (1988). *Nostoc* species in the field. *Algological Studies*, 50–53, 315–326.
- Montejano, Z. G., Cantoral-Uriza, E., & Carmona-Jiménez, J. (2004). Distribución de las algas de ambientes lóticos en la cuenca baja del río Pánuco [Distribution of algae from lotic environments in the lower basin of the Pánuco River]. In V. I. Luna, L. J. Morrone, & D. Espinosa (Eds.), *La Sierra Madre Oriental: Un enfoque multidisciplinario [The Sierra Madre Oriental: A multidisciplinary approach]* (pp. 111–126). CONABIO-Fac. Ciencias.
- Müller, J., Müller, K., Neinhuis, C., & Quandt, D. (2019). *PhyDE – Phylogenetic data editor* [software]. <http://www.phyde.de/>
- Necchi, O., Jr., Branco, L. H. Z., & Branco, C. C. Z. (1995). Comparison of three techniques for estimating periphyton abundance in bedrock streams. *Algological Studies*, 134, 393–402.
- Osorio-Santos, K., Pietrasiak, N., Bohunická, M., Miscoe, H. L., Kováčik, L., Martin, M. P., & Johansen, J. R. (2014). Seven new species of *Oculatella* (Pseudanabaenales, Cyanobacteria): Taxonomically recognizing cryptic diversification. *European Journal of Phycology*, 49, 450–470. <https://doi.org/10.1080/09670262.2014.976843>
- Pietrasiak, N., Johansen, J. R., Osorio-Santos, K., Shaligyn, S., & Martin, M. P. (2019). First insights into the population genetics of soil cyanobacteria with the description of a new genus:

- Myxocorys* gen. nov. and two species from the Americas. *Journal of Phycology*, 55, 976–996.
- Pietrasiak, N., Mühlsteinová, R., Siegesmund, M. A., & Johansen, J. R. (2014). Phylogenetic placement of *Symplocastrum* (Phormidiaceae, Cyanophyceae) with a new combination *S. californicum* and two new species: *S. flechtnerae* and *S. torsivum*. *Phycologia*, 53, 529–541. <https://doi.org/10.2216/14-029.1>
- Řeháková, K., Johansen, J. R., Casamatta, D. A., Xuesong, L., & Vincent, J. (2007). Morphological and molecular characterization of selected desert soil cyanobacteria: Three species new to science including *Mojavia pulchra* gen. et sp. nov. *Phycologia*, 46(5), 481–502.
- Reynolds, E. S. (1963). The use of lead citrate at a high pH as an electron opaque stain in electron microscopy. *Journal of Cell Biology*, 17, 208–221.
- Rodríguez-Flores, R., & Carmona-Jiménez, J. (2018). Ecology and distribution of macroscopic algae communities in streams from the Basin of Mexico. *Botanical Sciences*, 96(1), 63–75. <https://doi.org/10.17129/botsci.1237>
- Ronquist, F., Teslenko, M., Van Der Mark, P., Ayres, D. L., Darling, A., Höhna, S., Larget, B., Liu, L., Suchard, M. A., & Huelsenbeck, J. P. (2012). MrBayes 3.2: Efficient Bayesian phylogenetic inference and model choice across a large model space. *Systematic Biology*, 61, 539–542.
- Sabater, S., & Muñoz, I. (2000). *Nostoc verrucosum* (cyanobacteria) colonized by a chironomid larva in a Mediterranean stream. *Journal of Phycology*, 36, 59–61.
- Saraf, A. G., Dawda, H. G., & Singh, P. (2019). *Desikacharya* gen. nov., a phylogenetically distinct genus of cyanobacteria along with the description of two new species, *Desikacharya nostocoides* sp. nov. and *Desikacharya soli* sp. nov., and reclassification of *Nostoc thermotolerans* to *Desikacharya thermotolerans* comb. nov. *International Journal of Systematic and Evolutionary Microbiology*, 69(2), 307–315.
- Shalygin, S., Shalygina, R., Johansen, J. R., Pietrasiak, N., Berrendero, E., Bohunická, M., Mareš, J., & Sheil, C. (2017). *Cyanomargarita* gen. nov. (Nostocales, cyanobacteria): Convergent evolution resulting in a cryptic genus. *Journal of Phycology*, 53, 762–777. <https://doi.org/10.1111/jpy.12542>
- Southwood, T. R. E. (1978). *Ecological methods, with particular reference to the study of insect populations*. The English Language Book Society and Chopan-Hall.
- Siegesmund, M. A., Johansen, J. R., Karsten, U., & Friedl, T. (2008). *Coleofasciculus* gen. nov. (cyanobacteria): Morphological and molecular criteria for revision of the genus *Microcoleus* Gomont. *Journal of Phycology*, 44, 1572–1585. <https://doi.org/10.1111/j.1529-8817.2008.00604.x>
- Singh, P., Šnokhousová, J., Saraf, A., Suradkar, A., & Elster, J. (2020). Phylogenetic evaluation of the genus *Nostoc* and description of *Nostoc neudorfense* sp. nov., from the Czech Republic. *International Journal of Systematic and Evolutionary Microbiology*, 70(4), 2740–2749.
- Spurr, A. R. 1969. A low-viscosity epoxy resin embedding medium for electron microscopy. *Journal of Ultrastructure Research* 26, 31–43.
- Stackebrandt, E., & Ebers, J. (2006). Taxonomic parameters revisited: Tarnished gold standards. *Microbiology Today*, 33, 152–155.
- Thiers, B. M. (2023; continuously updated). *Index Herbariorum: A global directory of public herbaria and associated staff*. New York Botanical Garden's Virtual Herbarium. <https://sweetgum.nybg.org/science/ih/>
- Thompson, J. D., Higgins, D. G., & Gibson, T. J. (1994). Clustal W: Improving the sensitivity of progressive multiple sequence alignment through sequence weighting, position-specific gap penalties and weight matrix choice. *Nucleic Acids Research*, 22, 4673–4680. <https://doi.org/10.1093/nar/22.22.4673>
- Wilmotte, A., Van Der Auwera, G., & De Wachter, R. (1993). Structure of the 16S ribosomal RNA of the thermophilic cyanobacterium *Chlorogloeopsis* HTP (Mastigocladus laminosus HTF) strain PCC7518 and phylogenetic analysis. *FEBS letters*, 317, 96–100.
- Yarza, P., Yilmaz, P., Pruesse, E., Glöckner, F. O., Ludwig, W., Schleifer, K. H., Whitman, W. B., Euzéby, J., Amann, R., & Rosselló-Móra, R. (2014). Uniting the classification of culture and uncultured bacteria and Archaea using 16S rRNA gene sequences. *Nature Reviews Microbiology*, 12, 635–645.
- Zuker, M. (2003). Mfold web server for nucleic acid folding and hybridization prediction. *Nucleic Acids Research*, 31, 3406–3415.

SUPPORTING INFORMATION

Additional supporting information can be found online in the Supporting Information section at the end of this article.

Appendix S1

How to cite this article: Carmona Jiménez, J., Caro Borrero, A., Becerra-Absalón, I., Perona Urizar, E., Márquez Santamaría, K., & Mateo Ortega, P. (2023). Description of two new species of *Nostoc* (Nostocales, Cyanobacteria) from central Mexico, using morphological, ecological, and molecular attributes. *Journal of Phycology*, 59, 1237–1257. <https://doi.org/10.1111/jpy.13401>